



## Soft Foundation Strengthening Effect and Structural Optimization of a New Cement Fly-ash and Gravel Pile-slab Structure

D. B. Zhang<sup>a</sup>, Y. Zhang<sup>a,b</sup>, T. Cheng<sup>\*a</sup>, J. Y. Yuan<sup>a</sup>

<sup>a</sup> School of Civil Engineering, Hubei Polytechnic University, Hubei, China

<sup>b</sup> Department of Civil and Earth Resources Engineering, Kyoto University, Kyoto, Japan

### PAPER INFO

#### Paper history:

Received 22 December 2016

Received in revised form 02 March 2017

Accepted 21 April 2017

#### Keywords:

CFG pile-slab Structure  
Settlement  
Numerical Simulation  
Model Test

### ABSTRACT

Reducing the settlements of soft foundation effectively is a critical problem of high-speed railway construction in China. The new CFG pile-slab structure composite foundation is a ground treatment technique which is applied on CFG pile foundation and pile-slab structure composite foundation. Based on the experience of constructing Beijing-Shanghai high-speed railway in China, the settlement-controlling effect, the settlement distribution laws and three key influence factors for structural form of new CFG pile-slab structural foundation are studied by using physical model tests and numerical simulations. The research results in this study indicate that the piles and soil bearing capacities of the new CFG pile-slab structure can be put into full play because of the "load distributing" function of slabs. The settlement reducing effect of the new CFG pile-slab structure is remarkable and can meet the requirements of high-speed railway construction. The affected area of engineering load has a depth over 18.75 m and horizontal length of 7.5 m nearing the embankment slope toe. The parametric study provides the optimizing structural form for best settlement-controlling effect. The physical model test results show good concordance with the numerical simulation results. The combination of physical model tests and numerical simulations justifies the use of this model in geotechnical engineering practices.

doi: 10.5829/ije.2017.30.07a.04

### NOMENCLATURE

CFG	Cement Fly-ash Grave	$P$	External load
$\alpha_l$	Similarity constant of geometry	$\alpha_\sigma$	Similarity constant of stress
$\alpha_\epsilon$	Similarity constant of strain	$\alpha_E$	Similarity constant of elasticity modulus
$\alpha_\mu$	Similarity constant of poisson's ration	$\alpha_\phi$	Similarity constant of internal friction angle

### Greek Symbols

$w$	Water content (%)	$\gamma$	Specific weight (KN/m <sup>3</sup> )
$g$	Gravity (m/s <sup>2</sup> )	$E_s$	Elasticity modulus of soil (MPa)
$e$	Void ratio		

## 1. INTRODUCTION

With the rapid increasing traffic demands, more and more high-speed railways are being built in China. The allowable maximum settlement of Chinese high-speed railway is the most important key construction controlling factor in railway embankment construction

[1]. When building high-speed railway in coastal soft soil foundation, common foundation treatment technology cannot meet the settlement controlling requirement of high-speed railway. Therefore, the ground improvement techniques such as composite foundation are frequently adopted and studied in recent years [2-10]. Jiang et al. [11] presented a numerical analysis to investigate the pile-slab supported embankment, and the result shows the proportion of the

\*Corresponding Author's Email: 181816090@qq.com (T. Cheng)

load carried by the soil is small. Thus, it can significantly reduce the settlement and the stress transfer from the soil to the piles. Messioud et al. [12] presented a comparison between rigid piles and pile foundations. It has concluded the influence of the mattress stiffness, the geometrical configuration, and head/tip fixity conditions on the dynamic response of the foundation system. Han and Bhandari [13] studied the stresses and deformations of geogrid-reinforced embankments over piles. This study found the settlements of geogrid-reinforced embankments over geosynthetic piles are 20-30% smaller than pile supported embankments. Okyay et al. [4] presented a numerical analysis to analyze the impedance functions of slab foundations with rigid piles. The study has formulated the stress change laws for rigid piles. Chen et al. [14] discussed the influences of piling arrangement of the CFG pile composite foundation. The results show that the pile-soil stress ratio and the load-sharing ratio can be adjusted through setting up cushion thickness. Shen et al. [9] set up a three-dimensional simulation model of CFG pile foundation to investigate the influence of different cushion thicknesses on the deformation of CFG pile foundation. Moayed et al. [10] studied the minimum settlement which has tested various pile arrangements under different vertical stress levels. The results show that the arrangements of short and long piles become more effective when vertical stress on the raft increases.

Those researches show that the normal pile-slab structure (Figure 1) and CFG pile structure are both suitable for dealing with deep thick soft soil foundation. However, these structures will fail before the piles reach their bearing limits because of the large pile-soil stress ratio. In order to reduce the cost and improve the functionality of pile-slab structure and CFG pile structure, we developed this new type structure in this work, named new CFG pile-slab structure [15]. The new CFG pile-slab structure is constituted by CFG piles, reinforced concrete piles and reinforced concrete slab. The edge of each reinforced concrete slab is connected and supported by reinforced concrete piles into one nody. The middle of each reinforced concrete slab is connected and supported by CFG piles within one body (see Figure 2).

The Beijing - Shanghai high-speed railway connects the biggest city and the capital of China (see Figure 3). The design speed of high-speed trains is 350 km/h. Parts of the railway is constructed on a large area of soft soil foundation with very low bearing capacity and large potential settlements. In order to mitigate these potential risks, new CFG pile-slab structure are adopted. In this paper, physical model tests and numerical simulation are combined to investigate the settlement-controlling effect, the settlement distribution laws and the optimal structural style. The research aims to provide benefit for the design and construction of railway embankment.

## 2. ENGINEERING SITUATION

Part from Wuxi to Kunshan of the railway is constructed on a large area of soft soil foundation with very low bearing capacity and large potential settlements. We choose to apply the new CFG pile-slab structure for this area. Figures 4 and 5 show the floor plan view and cross-sectional view of this area for using the new CFG pile-slab structure. The railway embankment is 6.25 m high with a 1(V):1.5(H) side slopes. The thickness of soft soil layer is 5.1-9.7m.

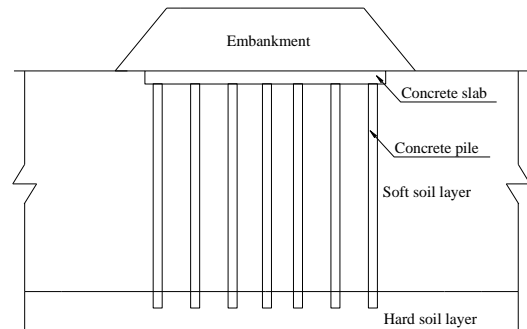


Figure 1. Illustration of normal pile-slab structure

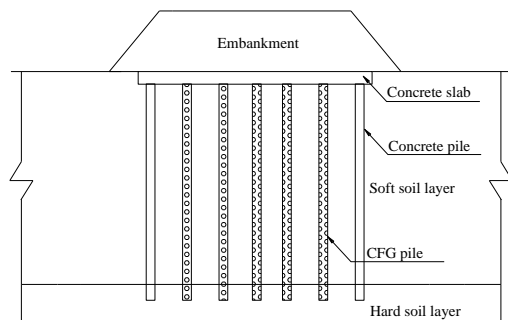


Figure 2. Illustration of new CFG pile-slab structure

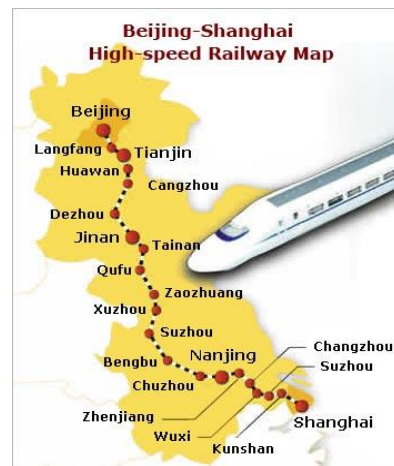


Figure 3. Map showing the high-speed railway from Beijing to Shanghai

The depth of investigated area is 25m and the width is 100m. The material of the embankment fill is well-graded sandy soil. A 0.8m-thick reinforced concrete slab is constructed under the embankment fill. Piles are directly covered by the reinforced concrete slab. The average soil properties are shown in Table 1.

**3. SIMILAR PHYSICAL MODEL TESTS**

**3.1. Similar Mechanical Properties** The study of similar principles is required to guarantee the similarity between the model and the prototype of CFG pile-slab structural foundation [16]. The geometric similarity constant is set to 25, and the other constants are calculated in two steps.

Step1. According to the similarity concept and the physical similarity of the model materials, the similarity constants which should be considered in the similarity analysis are given as follows:

$$a_\sigma = \frac{\sigma_H}{\sigma_M}, a_E = \frac{E_H}{E_M}, a_\varepsilon = \frac{\varepsilon_H}{\varepsilon_M} \tag{1}$$

$$E_H = \frac{\sigma_H}{\varepsilon_H} \tag{2}$$

$$E_M = \frac{\sigma_M}{\varepsilon_M} \tag{3}$$

where  $a_\sigma$  and  $a_E$  are the similarity constant of stress and deformation modulus, the subscript H represents the prototype and the subscript M represents the model.

By substitute formula 1 into formula 2, we can obtain:

$$a_E E_M = \frac{a_E \sigma_M}{a_\varepsilon \varepsilon_H} \tag{4}$$

Combining with formulae 3 and 4,  $a_E$  can be derived as:

$$a_E = \frac{a_\sigma}{a_\varepsilon}$$

Since  $\varepsilon$  is a dimensionless value and the similarity constant of deformation modulus equal the similarity constant of geometric dimension, so we have:

$$a_\varepsilon = 1, a_\sigma = a_E = a_l = 1$$

Step 2. The similarity ratio is calculated by the influence factors of structural deformation. Because the structural stress is related to load, deformation modulus of the material, material Poisson's ratio, and the structural size, the relationships between stress, displacement in the structure and other variables can be expressed as:

$$f(\sigma, F, q, \gamma, l, E, \mu, p, S) = 0 \tag{5}$$

where  $F$  is the surface load,  $q$  is the line load,  $\gamma$  the material bulk density,  $l$  the structural size,  $E$  the Deformation modulus,  $\mu$  the Poisson's ratio,  $p$  the reinforcement ratio,  $\sigma$  the structural stress, and  $S$  the displacement.

There are nine irrelevant variables in formula 5 and two of them are independent variables ( $F, l$ ). Based on the factor analysis, the 7 dimensionless quasi-numbers can be written as:

$$\Pi_1 = \frac{p}{F^{a_1} l^{b_1}}, \Pi_2 = \frac{\mu}{F^{a_2} l^{b_2}}, \Pi_3 = \frac{E}{F^{a_3} l^{b_3}}, \Pi_4 = \frac{\gamma}{F^{a_4} l^{b_4}}, \tag{6}$$

$$\Pi_5 = \frac{q}{F^{a_5} l^{b_5}}, \Pi_6 = \frac{\sigma}{F^{a_6} l^{b_6}}, \Pi_7 = \frac{S}{F^{a_7} l^{b_7}} \tag{7}$$

Again, according to the factor analysis, the dimension equation of  $\Pi_1$  are derived as follows:

$$[0] = [MLT^{-2}]^{-a_1} [L]^{b_1} \left. \begin{matrix} M & a_1 = 0 \\ L & a_1 + b_1 = 0 \\ T & -2a_1 = 0 \end{matrix} \right\} \tag{8}$$

Then solution of formula 8 can be obtained as:

$$a_1 = 0, b_1 = 0, \Pi_1 = p$$

The other dimension equations can be solved in the same way.

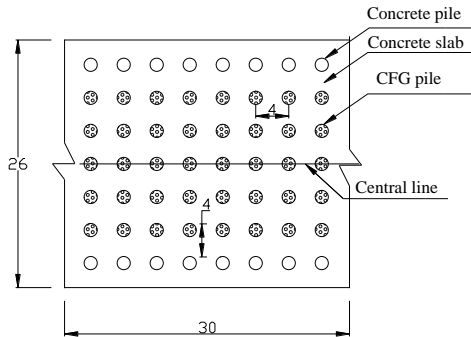


**Figure 4.** Floor plan view of new CFG pile-slab structure (unit: m)

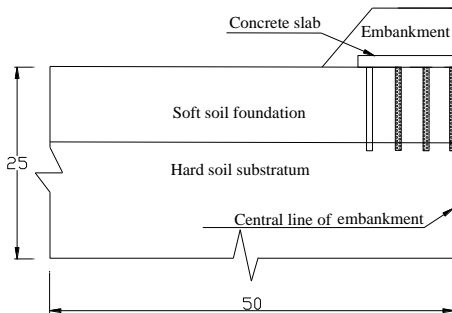


**Figure 5.** Cross-sectional view of study area (unit: m)

$$\Pi_2 = \mu, \Pi_3 = \frac{El^2}{F}, \Pi_4 = \frac{\gamma l^3}{F}, \Pi_5 = \frac{ql}{F}, \Pi_6 = \frac{\sigma l^2}{F}, \Pi_7 = \frac{Sl}{F}$$

Then formula 5 can be rewritten as:

$$f\left(F, l, p, \mu, \frac{El^2}{F}, \frac{\gamma l^3}{F}, \frac{ql}{F}, \frac{\sigma l^2}{F}, \frac{Sl}{F}\right) = 0 \tag{9}$$

According to the conclusions of step 1 and the principle of factor analysis, the similarity constants for real size prototype versus physical model can be calculated as follows:

$$\alpha_\mu = \alpha_p = \alpha_\varepsilon = 1 \tag{10}$$

$$\alpha_F = \alpha_E \alpha_l^2 = \alpha_l^2 \tag{11}$$

$$\alpha_\gamma \alpha_l^3 = \alpha_F = \alpha_l^2 \alpha_E, \alpha_\gamma = \frac{1}{\alpha_l} \tag{12}$$

$$\alpha_q = \alpha_l = \alpha_s = 1 \tag{13}$$

$$\alpha_1 = \frac{x_p}{x_m} = \frac{y_p}{y_m} = \frac{z_p}{z_m} = \frac{u_p}{u_m} = \frac{v_p}{v_m} = \frac{\omega_p}{\omega_m} = \frac{l_p}{l_m} \tag{14}$$

$$\alpha_\sigma = \frac{(\sigma_x)_p}{(\sigma_x)_m} = \frac{(\sigma_y)_p}{(\sigma_y)_m} = \frac{(\sigma_z)_p}{(\sigma_z)_m} = \frac{(\tau_{xy})_p}{(\tau_{xy})_m} = \dots = \frac{\sigma_p}{\sigma_m} \tag{15}$$

$$\alpha_\varepsilon = \frac{(\varepsilon_x)_p}{(\varepsilon_x)_m} = \frac{(\varepsilon_y)_p}{(\varepsilon_y)_m} = \frac{(\varepsilon_z)_p}{(\varepsilon_z)_m} = \frac{(\gamma_{xy})_p}{(\gamma_{xy})_m} = \dots = \frac{\varepsilon_p}{\varepsilon_m} \tag{16}$$

$$\alpha_E = E_p / E_m \tag{17}$$

$$\alpha_\mu = \mu_p / \mu_m \tag{18}$$

$$\alpha_\phi = \mu_\phi / \mu_\phi \tag{19}$$

Based on the aboved formulas, the values of each similarity constants are calculated and shown in Table 2.

Through more than 700 times material mechanical experiment tests, the similar material of model test is developed. The main ingredients are concrete, gypsum, barite powder and quartz sand [16]. Main physical and mechanical parameters of similar materials are recorded in Table 3.

**3. 2. Test Apparatus** Test apparatus is composed of model box, loading system and monitoring system. The model tests take place in a model box which is welded into a framework by angle steels. In real practice, CFG piles are installed into nearly 10 m below the ground surface which is deeper than the soft soil layers. But the other soil layers are extended to nearly 90 m deep. In the loading system, based on the similarity constants, the size of the simulated structure is 25 times smaller than the real structure.

TABLE 1. Average soil properties

Soil layer	Unit weight (kN/m <sup>3</sup> )	Water content (%)	Liquid limit (%)	Plastic limit (%)	Deformation modulus (MPa)
Soft soil	18	41.9	48	26.8	15.9
Hard soil	21.4	23.4	33.7	20.2	26.5
Embankment fill	23.6	21.2	28.9	17.5	29.2

TABLE 2. Similarity constants of prototype versus physical model

Similarity constants	Value	Similarity constants	Value
Geometric dimension	25	Stress	1
Unit weight	1	Load on surface	625
Deformation modulus	25	Deformation	25
Poisson's ratio	1	Strain	1
Internal friction angle	1	Bearing capacity	625

TABLE 3. Main physical and mechanical parameters of similar materials

Types	Deformation modulus (MPa)		Poisson's ratio		Internal friction angle (o)		Cohesion (kPa)	
	Prototype	Model	Prototype	Model	Prototype	Model	Prototype	Model
Concrete slab	20000	800	0.16	0.16	—	—	—	—
Concrete pile	18000	720	0.20	0.20	—	—	—	—
CFG pile	12000	480	0.21	0.21	—	—	—	—
Soft soil	15.9	0.636	0.32	0.32	21.3	21.3	17.3	0.692
Hard soil	26.5	1.06	0.28	0.28	24.7	24.7	12.4	0.496
Embankment soil	31.2	1.248	0.26	0.26	26.5	26.5	9.5	0.38

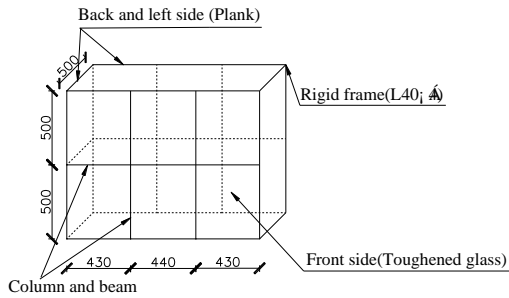


Figure 6. Framework of model box

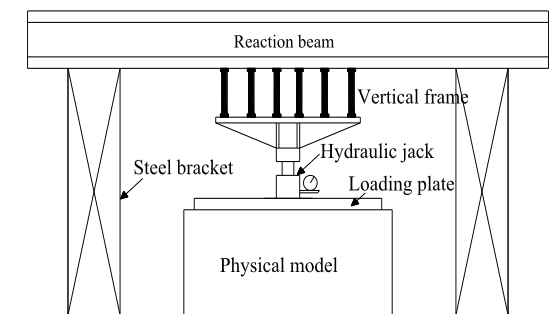


Figure 7. Loading system of model test

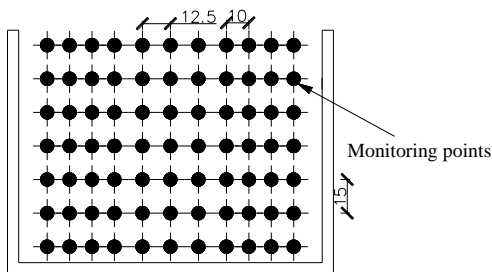


Figure 8. The arrangement of monitoring points (unit: cm)

Monitoring system is composed of arrangement of monitoring points, dial indicators and the close-shot photography measure system [17, 18]. Close-shot photography is a non-contact method to measure the total and local deformation changes of soil specimens during a test. The method is simple and cost-effective, requiring only a commercial digital camera to take pictures of a specimen from which accurate pixel model of the soil specimen is reconstructed. The deformation of each monitoring points can be obtained based on the changes of pixel coordinates [19]. The close shot photography measure system is adopted to monitor the deformation of the whole model and the dial indicators are adopted to monitor the deformation of piles in different testing stage. The arrangement of monitoring points are shown in Figure 8.

#### 4. RESULTS AND DISCUSSIONS

**4. 1. Settlements of Single Pile** Figures 9 and 10 present the settlements curves of CFG and concrete piles separately. From the curves, it can be concluded that the bearing capacity of both single CFG pile and single reinforced concrete pile are more than 350 kPa which is enough to take the maximum load per unit area by high-speed trains.

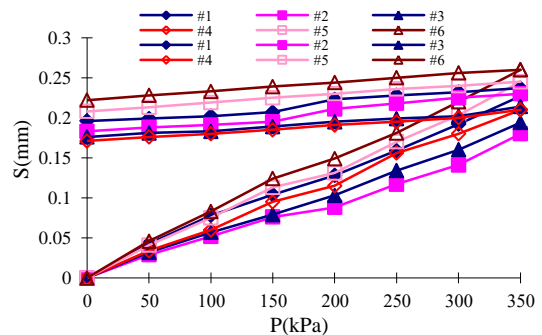


Figure 9. The settlement curves of single CFG pile

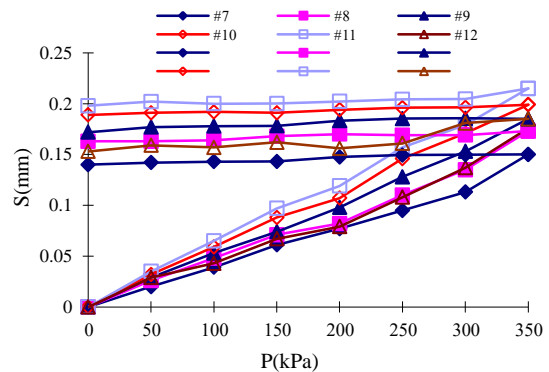


Figure 10. The settlement curves of single concrete pile

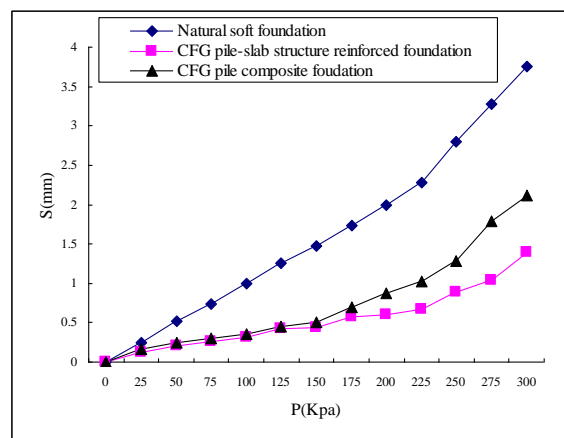


Figure 11. The settlement curves of natural foundation, CFG pile-slab structural foundation, and CFG pile composite foundation

Under the same external loads, the settlements of CFG piles are larger than reinforced concrete piles because of smaller deformation modulus. CFG piles and reinforced concrete piles carried most of the external pressure. Both kinds of piles are rigid and the bearing capacity are far more than the biggest external pressure. But after unloading the external pressure, the resilience rate of both the two kinds of piles are low.

**4. 2. Settlement Controlling Effect** The comparative analysis between the settlement of natural foundation, CFG pile composite foundation and new CFG pile-slab structure reinforced foundation is shown in Figure 11. It can be known that the maximum settlement of natural foundation is much bigger than the maximum settlement of CFG composite foundation. And maximum settlement of CFG composite foundation is bigger than the maximum settlement of new CFG pile-slab structure for the same external loads. In the model tests, the new CFG pile-slab structure can reduce the settlement of natural foundation from 3.75 mm to 1.38 mm when the maximum pressure on the foundation is 300 kPa. Figure 14 also shows that when the stress is smaller than 175 kPa, the settlements of CFG composite foundation are nearly the same as that of new CFG pile-slab structure. But, when the stress is bigger than 175 kPa, the settlements show large difference between the two kinds of foundations. This is the reason why without the distribution effect of slab, the pile-soil stress ratios of CFG composite foundation are bigger than new CFG pile-slab structure. More external loads are distributed on the piles. According to the geometric similar ratio, the maximum settlement of natural foundation is 93.75 mm, and that of CFG composite foundation is 52.63 mm, whereas the maximum settlement of the same foundation adopting new CFG pile-slab structure is only 34.5 mm. It can be concluded that the settlement controlling effect of new CFG pile-slab structure on soft soil foundation is remarkable.

#### 4. 3. Settlement Effects on the Ground Soil

Figure 12 shows the settlement curves versus external force of CFG pile-slab structural foundation. The measured points are at the middle of the model in horizontal direction while under the model surface from 0-90 cm in vertical direction. Figure 12 also shows that the settlements are increasing linearly with the test pressure when the test pressure is lower than 200 kPa. The settlements are increasing even faster when the test pressure is higher than 200 kPa. It can be concluded that the loading process can be divided into an elastic deformation phase and a ductile deformation phase. The settlement value of the surface is biggest, but the value is still less than the allowable maximum settlement based on the Chinese Technical Code for Ground Treatment for railway construction. The settlement

values at the middle of model in horizontal direction are decreasing with the increase of soil depth under the same test pressure. The test pressure produced no effect on ground soil when the depth is more than 90cm under the model surface.

Figure 13 shows the settlement curves of measured points of CFG pile-slab structural foundation when the test pressure is 300 kPa. The measured points are at different depths in horizontal direction and different planimetric position in vertical direction. Figure 13 also shows the settlements of the points, which are at the different depths of model, are decreasing with the distance to the embankment slope toe. The settlement values at the depth more than 75 cm remain unchanged when the distances to the embankment slope toe are more than 30 cm. Therefore, it implies the test pressure has less effect on ground soil when the depth is more than 75 cm and the horizontal distances to the embankment slope toe are more than 30 cm. According to the geometric similar ratio, the settlement affected an area having depth of 18.75 m and horizontal distance of 7.5 m around the embankment slope toe. It can be concluded that the settlement soil outside the embankment is under control and the soil is still in elastic deformation phase.

## 5. NUMERICAL SIMULATION

**5. 1. Model's Calculation Scheme** A three-dimensional model is created to simulate the behavior of the CFG pile-slab structural foundation using ANSYS 17.0 software. Due to the symmetry of this model, the left half of the model is selected (see Figures 4 and 5). The length of the numerical model are consistent with the slab. In order to ignore bottom and horizontal boundaries effect on the numerical results, the numerical model is extended to 25 m deep and 50m wide, which is approximately 4 times the depth and width of half embankment. Main material properties of different parts in the numerical model are shown in Tables 1 and 3.

The mechanical boundary conditions have been set as follows: the bottom displacements are fixed in both horizontal and vertical directions; the horizontal displacements on the left and right sides are set as fixed. The left and right side boundary of the numerical model are assumed impervious because the water could drain out freely at the surface of ground. The bottom boundary of the numerical model is also assumed impervious because of the low permeability soil layers.

**5. 2. Settlement Analysis and Comparisons** In order to validate the reliability of model test in settlements controlling effect, the settlement contrast curves between CFG pile-slab structural foundation and natural foundation are drawn by numerical results.

Figures 14, 15 and 16 show that under the same test pressure, the maximum settlement of natural soft foundation is approximately 93.8 mm while the maximum settlement of CFG pile-slab structure reinforced foundation is approximately 37.2mm. The settlement pictures of both the natural soft foundation and CFG pile-slab structure reinforced foundation show some parallel “U” shapes and decreasing with the increase of soil depth. Figure 14 also shows the maximum settlement of new CFG pile-slab structure reinforced foundation is smaller than the admissible settlement value of high-speed railway of China. Soft foundation reinforced by CFG pile-slab structure could completely meet the settlement requirement of high-speed railway constructions. The result of model test and numerical simulation are nearly the same.

**5. 3. Parametric Study of Structural Form** To further investigate the performance of the settlement change law of new CFG pile-slab structural foundation, 3 key influence factors are selected for the parametric study of structural form in the following discussion.

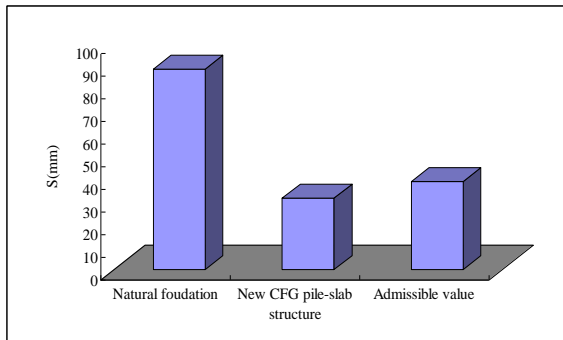


**Figure 14.** The contrast picture of ground subsidence when  $p=300\text{kPa}$

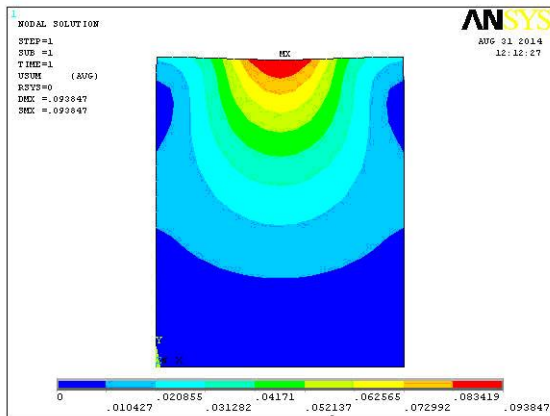


**Figure 15.** The settlement distributions of natural soft foundation when  $p=300\text{kPa}$

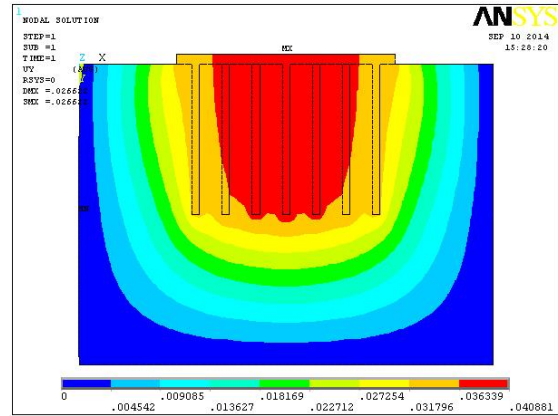


**Figure 16.** The settlement distributions of new CFG pile-slab structure reinforced foundation when  $p=300\text{kPa}$

These include pile length, pile diameter and slab thickness.

**5. 3. 1. Influence of Pile Length** The average pile length for the study is increased from 5 m to 21 m. Figure 17 shows the settlements of new CFG pile-slab structural foundation at different pile length while the external pressure is 300 kPa. And the pile diameter and slab thickness are constant values. It is shown that the settlement at the foundation surface and pile bottom layer are both decreasing dramatically with the increase of slab thickness. Figure 17 also shows the settlement at the foundation surface and pile bottom layers are very close. This is because the slab, piles and soils have a good coordination for settlement controlling. With the increasing of the pile lengths, the piles transfer the external loads to deeper and harder layers; the end-bearing force and friction of piles are also increasing. When the pile lengths exceed 15 m, the settlement controlling effect are not dramatical anymore. It means that there exists an optimizing pile length for the CFG pile-slab structure.

**5. 3. 2. Influence of Pile Diameter** The average pile diameter in the study is increased from 0.3 m to 1 m. Figure 18 shows the settlement of new CFG pile-slab structural foundation at different pile diameters while the external pressure is 300 kPa. The pile length is 15m and slab thickness is set at constant value. The study results show that along with the pile diameter increasing, the settlement controlling effect of new CFG pile-slab structure composite foundation is better and better, but when the pile diameter exceeds 0.6 m, the settlement controlling effect becomes less obvious. With the increasing of the pile diameters, both the friction of piles and the bearing capacity of piles are increasing. The loads distributed on the soil are decreasing, so the bearing capacity of CFG pile-slab structure is reinforced

and the settlements are decreased. It is concluded that there exists an optimizing pile diameter for the CFG pile-slab structure.

**5.3.3 Influence of Slab Thickness** The lengths of the piles are assumed to be 15 m and the diameters are assumed to be 0.6 m. The average slab thickness in the numerical analysis is increased from 0.2 m to 1.0 m. Figure 19 shows the settlement curves of new CFG pile-slab structural foundation at different slab thickness while the external pressure is 300 kPa. It is shown that the settlements at the foundation surface and pile bottom layer are both slightly decreased with the increase of slab thickness.

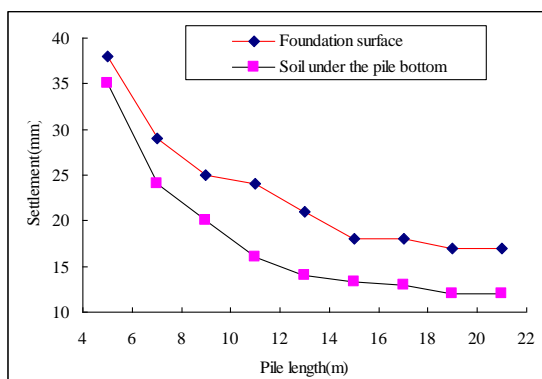


Figure 17. The settlement curves of different pile length

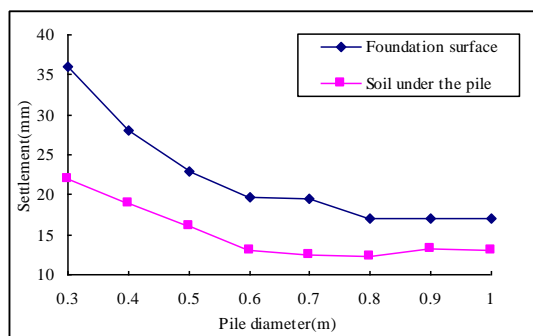


Figure 18. The settlement curves of different pile diameter

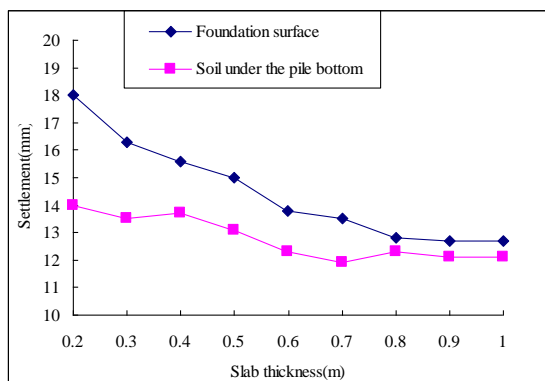


Figure 19. The settlement curves of different slab thickness

When the slab thickness is larger than 0.8 m, the settlements at the foundation surface is close to the pile bottom layer, the settlement controlling of the CFG pile-slab structural foundation is not significant. That is because the increase in the slab thickness can slightly reduce the differential settlement of the central slab. With the increasing of the slab thicknesses, the slab flexibility can be increased, and therefore the slab can distribute the outside load.

According to the above study on the 3 influencing factors of settlements, it can be concluded that selecting proper structural type is a very good way to adjust the sharing load between pile and soil and reducing the foundation settlements, which can finally help to achieve the purpose of optimized design.

## 6. CONCLUSION

1) The similar physical model test and numerical simulation model can adequately predict the performance of the CFG pile-slab structural foundation. The test results show good concordance with the numerical results.

2) The average settlement of CFG pile-slab supported soft foundation is less than the natural soft foundation on the same conditions. Reinforced concrete piles and CFG piles carry most of the external embankment loads, the combination of the piles and reinforced concrete slab can significantly reduce the vertical stresses applied onto the soils between piles.

3) The settlements of CFG pile-slab supported soft foundation are decreasing with the vertical depth and horizontal distance to the embankment slope toe. The engineering load could affect a depth of 18.75 m and width of 7.5 m around the embankment slope toe.

4) The optimal size of the new CFG pile-slab structure are 15 m for pile length, 0.6 m for pile diameter, and 0.8 m for slab thickness. When constructing the CFG pile-slab structure utilizing the optimal size, both the bearing capacity of pile and soil can be put into full play because of the "load distributing" function of slab.

## 7. ACKNOWLEDGEMENTS

The authors gratefully acknowledge the financial support of Natural Science Foundation of Hubei Province (2015CFB359) and Outstanding Young Innovative Team of Hubei Polytechnic University (14xjz01A).

## 8. REFERENCES

- Zhan, Y.-x., Yao, H.-l. and Jiang, G.-l., "Design method of pile-slab structure roadbed of ballastless track on soil subgrade",

- Journal of Central South University*, Vol. 7, No. 20, (2013), 2072-2082.
- Abusharar, S.W., Zheng, J.-J. and Chen, B.-G., "Finite element modeling of the consolidation behavior of multi-column supported road embankment", *Computers and Geotechnics*, Vol. 36, No. 4, (2009), 676-685.
  - Chen, R., Chen, Y., Han, J. and Xu, Z., "A theoretical solution for pile-supported embankments on soft soils under one-dimensional compression", *Canadian Geotechnical Journal*, Vol. 45, No. 5, (2008), 611-623.
  - Okay, U., Dias, D., Billion, P., Vandeputte, D. and Courtois, A., "Impedance functions of slab foundations with rigid piles", *Geotechnical and Geological Engineering*, (2012), 1-12.
  - Beer, M., Zhang, Y., Quek, S.T. and Phoon, K.K., "Reliability analysis with scarce information: Comparing alternative approaches in a geotechnical engineering context", *Structural Safety*, Vol. 41, (2013), 1-10.
  - Shooshpashaa, I., Mola-Abasia, H. and Amirib, I., "Evaluation of static and dynamic methods for determining the bearing capacity of the driven pipe piles", *International Journal of Engineering*, Vol., No. 2, (2014), 27-35.
  - Kermani, H., Behnamfar, F. and Morsali, V., "Seismic design of steel structures based on ductility and incremental nonlinear dynamic analysis", *International Journal of Engineering-Transactions A: Basics*, Vol. 29, No. 1, (2015), 23-30.
  - Huang, J. and Han, J., "Two-dimensional coupled hydraulic and mechanical modeling of geosynthetic-reinforced column-supported embankments", *Comput Geotech*, Vol. 37, (2010), 638-648.
  - Shen, Y. and Wang, H., "Optimization design on cfg-pile foundation with different cushion thickness in beijing-shanghai high-speed railway", *Transportation Infrastructure Geotechnology*, Vol. 3, No. 1, (2016), 3-11.
  - Moayed, R.Z., Izadi, E. and Mirsepahi, M., "3d finite elements analysis of vertically loaded composite piled raft", *Journal of Central South University*, Vol. 6, No. 20, (2013), 1713-1723.
  - Jiang, Y., Han, J. and Zheng, G., "Numerical analysis of a pile-slab-supported railway embankment", *Acta Geotechnica*, Vol. 9, No. 3, (2014), 499-507.
  - Messiod, S., Okay, U.S., Sbartai, B. and Dias, D., "Dynamic response of pile reinforced soils and piled foundations", *Geotechnical and Geological Engineering*, Vol. 3, No. 34, (2016), 789-805.
  - Han, J., Bhandari, A. and Wang, F., "Dem analysis of stresses and deformations of geogrid-reinforced embankments over piles", *International Journal of Geomechanics*, Vol. 12, No. 4, (2011), 340-350.
  - Chen, Q.-n., Zhao, M.-h., Zhou, G.-h. and Zhang, Z.-h., "Bearing capacity and mechanical behavior of cfg pile composite foundation", *Journal of Central South University of Technology*, Vol. 15, (2008), 45-49.
  - Zhang, D., Zhang, Y., Cheng, T. and Yuan, J., "New analytic method for subgrade settlement calculation of the new cement fly-ash grave pile-slab structure", *International Journal of Engineering-Transactions A: Basics*, Vol. 29, No. 10, (2016), 1364-1372.
  - Ding-Bang, Z., Chuan-bob, Z., Yang-bob, L. and Jian-yia, Y., "Physical model test and numerical simulation study of deformation mechanism of wall rock on open pit to underground mining", *International Journal of Engineering Transactions B Applications*, Vol. 27, No. 11, (2014), 1795-1802.
  - Habib, A.F., Morgan, M. and Lee, Y.R., "Bundle adjustment with self-calibration using straight lines", *The Photogrammetric Record*, Vol. 17, No. 100, (2002), 635-650.
  - Xin, L., Shu-wen, L., Shu-gen, W. and Wei-zhong, R., "Application of digital close range photogrammetry in physical model deformation measurement of highway slope", *Science of Surveying and Mapping*, Vol. 5, (2011), 078.
  - Ding-bang, Z., Yi, Z., Tao, C., Yuan, M., Kun, F., Ankit, G. and Akhil, G., "Measurement of displacement for open pit to underground mining transition using digital photogrammetry", *Measurement*, (2017), 132-140.

## Soft Foundation Strengthening Effect and Structural Optimization of a New Cement Fly-ash and Gravel Pile-slab Structure

D. B. Zhang<sup>a</sup>, Y. Zhang<sup>a,b</sup>, T. Cheng<sup>a</sup>, J. Y. Yuan<sup>a</sup>

<sup>a</sup> School of Civil Engineering, Hubei Polytechnic University, Hubei, China

<sup>b</sup> Department of Civil and Earth Resources Engineering, Kyoto University, Kyoto, Japan

### PAPER INFO

چکیده

#### Paper history:

Received 22 December 2016

Received in revised form 02 March 2017

Accepted 21 April 2017

#### Keywords:

CFG pile-slab Structure

Settlement

Numerical Simulation

Model Test

Optimum Parameters

Isotherms

کاهش نشست فونداسیون‌های نرم یک مشکل مهم در ساخت و ساز راه آهن با سرعت بالا در چین است. اساس کامپوزیت با ساختار جدید CFG، یک روش بهبود زمین است که بر پایه شمع‌های ورقه‌ای CFG و فونداسیون‌های کامپوزیت ساختاری شمع ورقه‌ای اعمال می‌شود. بر اساس تجربه ساخت راه آهن با سرعت بالا بین پکن و شانگهای در چین، تاثیر کنترل نشست، قوانین توزیع بار و سه عامل کلیدی موثر برای شکل ساختاری شمع‌های ساختاری جدید CFG جدید با استفاده از آزمون‌های مدل فیزیکی و شبیه سازی عددی بررسی شده است. نتایج این تحقیق نشان می‌دهد که حد اکثر استفاده از ظرفیت‌های شمع‌ها و تحمل خاک ساختار شمع جدید CFG به علت عملکرد توزیع بار شمع‌ها به دست می‌آید. اثر کاهش نشست شمع CSG جدید قابل توجه است و می‌تواند نیازهای ساخت و ساز راه آهن با سرعت بالا را تامین کند. منطقه آسیب دیده از بار مهندسی عمق بیش از ۱۸٫۷۵ متر و طول افقی ۷٫۵ متر در نزدیکی پاشنه فونداسیون است. مطالعه پارامتریک، شکل ساختاری بهینه برای بهترین اثر کنترل استقرار را فراهم می‌کند. نتایج آزمون‌های مدل فیزیکی نشان می‌دهد که سازگاری خوبی با نتایج شبیه سازی عددی دارد. ترکیبی از آزمون‌های مدل فیزیکی و شبیه سازی‌های عددی، استفاده از این مدل را در شیوه های مهندسی ژئوتکنیک توجیه می‌کند.

doi: 10.5829/ije.2017.30.07a.04